Microelectronic Engineering 88 (2011) 969–975

Contents lists available at ScienceDirect

Microelectronic Engineering

journal homepage: www.elsevier.com/locate/mee

Investigation of barrier inhomogeneities in Mo/4H–SiC Schottky diodes

L. Boussouar [a], Z. Ouennoughi [a,*], N. Rouag [a], A. Sellai [b], R. Weiss [c], H. Ryssel [c]

[a] Laboratoire optoélectronique et composants, UFAS Sétif, Algeria
[b] Physics Department, P.O. Box 36, Sultan Qaboos University 123, Oman
[c] FIIS, Schottkystrasse 10, 91058 Erlangen, Germany

ARTICLE INFO

Article history:
Received 21 May 2010
Received in revised form 19 December 2010
Accepted 23 December 2010
Available online 30 December 2010

Keywords:
4H–SiC
Schottky diodes
Current–voltage characteristics
Barrier inhomogeneities

ABSTRACT

Using current–voltage measurements, we have investigated the electrical behavior of molybdenum on 4H–SiC Schottky diodes of various areas and having different edge terminations consisting of high resistivity guard rings manufactured by carbon ion-implantation.

Both forward and reverse electrical characteristics of Schottky contacts indicated a presence of inhomogeneities.

The forward *I–V* characteristics have been primarily analyzed within the framework of a standard thermionic emission theory. Schottky-barrier heights and ideality factors are found to appreciably vary from diode to diode. A more general model which takes into account the inhomogeneity of the Schottky barrier has been then used to extract the parameters pertinent to the barrier height distribution. The description of the experimental results using Tung's model allowed us to determine the value of the average laterally homogeneous SBH barrier height between 1.2 and 1.39 *eV* for Mo/4H–SiC Schottky diodes. The patch's properties (the number of patches, the patch strength and the local series resistance) were also obtained from the fit to the experimental *I–V* characteristics of the current through "patchy" diodes. The obtained results are best described with this extended "pinch off" model.

With respect to the reverse characteristics, the remarked absence of a non-saturating behavior as a function of bias in the experimental reverse-bias branch may well be attributed to the presence of defects and/or inhomogeneous Schottky barrier heights, associated with the non-ideal contacts.

1. Introduction

The 4H–SiC Schottky barrier diodes (SBDs) are attractive devices for high temperature, high frequency and high power electronics [1,2]. Various metals have been used for the formation of Schottky contacts on *n*-type 4H–SiC by many research groups [3–12]. Thermally stable Schottky contacts is a requirement for better performance SiC based devices, and for this reason refractory and noble metals are the materials of choice used for making both ohmic and Schottky contacts.

Recently, a number of publications have reported the use of molybdenum (Mo) for fabrication of high-performance Schottky devices [4,8,13–17]. Using *C–V* measurements, Yakimova et al. [4] reported Schottky barrier heights of the order of 1.03 and 1.28 *eV*. Nakamura et al. [14] prepared SBDs using Mo contacts followed by annealing at a high temperature, derived a barrier height of 1.2–1.3 *eV* from *I–V* measurements and reported no degradation in the ideality factor nor in the reverse characteristics. Similarly, Mo/4H–SiC diodes fabricated by Vassilevski et al. [15] revealed unchanging ideality factor and barrier height (1.21–1.3 *eV*) at temperature up to 400 °C.

In a previous study [8], molybdenum SBDs have been fabricated with different edge termination and the investigation and discussion, in that work, was restricted to the effect of ion implantation induced high resistivity guard ring structures on the behavior of the Schottky diodes.

In the present work, we report a detailed analysis of the electrical behavior of molybdenum Schottky diodes on 4H–SiC with different areas and with different edge termination.

The *I–V* characterization of the Schottky diodes under forward and reverse bias was performed in order to determine the significant parameters ruling the current transport across the metal/4H–SiC contact.

The Mo/4H–SiC diodes under study exhibit a forward characteristic that is in good agreement with thermionic emission theory. However, the experimentally obtained values for the SBHs are much lower than those predicted by the Schottky–Mott relation, with the ideality factors close to unity. The electrical characteristics were, subsequently, discussed in the framework of the existing model on inhomogeneous barriers proposed by Tung [18]. When Schottky barrier parameters are re-evaluated using this model instead of the pure thermionic diffusion model, values much more

* Corresponding author. Tel.: +213 36839612.
E-mail addresses: ouzahir@univ-setif.dz, ouennoughi@gmail.com (Z. Ouennoughi).

0167-9317/$ - see front matter © 2010 Elsevier B.V. All rights reserved.
doi:10.1016/j.mee.2010.12.070

consistent with previously published data on Mo/4H–SiC diodes [14–17] were obtained. Also, a correlation between the number of patches N_p (defects) and the carbon implantation dose will be shown.

For the reverse characteristic, it is particularly noted that the leakage current was some orders of magnitudes higher than predicted by the thermionic emission theory. Crystal defects in SiC wafers are considered to be responsible for this high observed leakage current.

2. Device fabrication and characterization

The substrate material used for the Schottky diodes was *n*-type 4H–SiC (0001) from Cree Inc. with a 10 μm epitaxial-layer with a donor concentration in the range of 8.0×10^{15} to $1.3 \times 10^{16}\,cm^{-3}$. A 42 nm thick oxide layer thermally grown on the epitaxial-layer served both as passivation layer for regions around the Schottky contact and as a sacrificial layer for regions where the contacts were formed. An additional 240 nm thick layer of SiO_2 was deposited by LPCVD. The oxide layer was structured by photolithography. The ion implantation of carbon at different energies and doses for the formation of the guard rings was done at room temperature. Schottky contacts were formed by depositing, through e-beam evaporation, molybdenum on the SiC substrate at a pressure of approximately $1 \times l0^{-5}$ Pa followed by annealing in an open furnace at 500 °C under a N_2 flow of about 1000 sccm. A backside ohmic contact was formed by e-beam deposition of 2500 Å of molybdenum, followed by an anneal at about 1070 °C in a vacuum furnace. After the formation of the Schottky contacts, an anneal was carried out in an open furnace at 500 °C. Fig. 1 shows a schematic cross section of a Schottky diode. The two main geometrical parameters of the Schottky diodes are the diode (D) diameter and the guard ring width (W). The Schottky contacts had a circular geometry with diameters varying from 150 to 300 μm and the width of the guard ring varying from 50 to 150 μm. The high resistivity layer forming the guard ring was generated by carbon ion implantation at four different doses: 1.2×10^{12}, 7×10^{12}, 3.5×10^{13} and $1.75 \times 10^{14}\,cm^{-2}$. Table 1 shows the different parameters of the fabricated diodes. The *I–V* measurements were performed with a Keithley 237 Source and Measurement Unit which is capable of handling voltages up to 1100 V. The electrical *I–V* measurements of the Schottky diodes were made in the temperature range of 303–498 K with a step of 25 K because SiC Schottky diodes are generally intended to operate at elevated temperatures. It has to be noted that in our *I–V–T* measurements the typical reading error in the current is less than 1% and the temperature is determined with accuracy better than 0.1 K.

Table 1
Geometrical characteristics of the Schottky diodes.

Group diode	D (μm)	W (μm)
I	150	50
		60
		75
II	200	50
		75
		100
III	300	50
		100
		150

3. Results and discussion

3.1. Reverse characteristics

More than 60 diodes were characterized at room temperature. The experimental *I–V* curves reported in this paper were chosen as representative of the general electrical trend of the contact. Typical reverse characteristics of the studied diodes are shown in Figs. 2 and 3. The shape of the reverse *I–V* curves is similar to those reported earlier for Mo Schottky devices on 4H–SiC [14–16]. The reverse breakdown voltages were observed at voltage above 400 V at carbon dose of $1.2 \times 10^{12}\,cm^{-2}$ and above 800 V at carbon dose of $1.75 \times 10^{14}\,cm^{-2}$ as shown in Fig. 2a and b.

It has been observed, that the reverse breakdown voltage also increases with decreasing contact area. The same behavior has been observed on Ni/SiC Schottky diodes with junction termination extension [19,20]. This is most likely due to increased probability of having crystal defects in active region as the area increased. In 4H–SiC, defects such as micropipes, and screw dislocations [20,21] are among the responsible factors for the high leakage current observed in SiC Schottky diodes. The nature of the surface surrounding the metal contact is also invoked to be responsible for the large variation of this leakage current [22].

The fact that the measured leakage current is several orders of magnitude larger than predicted by thermionic emission theory has also been observed for 4H–SiC Schottky diodes [5–7,15,16,19,23–25] and has been explained by several mechanisms such as combination of thermionic field emission and field emission [23], quantum–mechanical tunneling [24] or barrier height inhomogeneity [26]. SiC Schottky diodes utilize edge termination in order to reduce surface leakage current and increases breakdown voltage near the device edge.

No clear correlation between the width of the guard ring and the reverse characteristics of the Mo/4H–SiC diodes was observed.

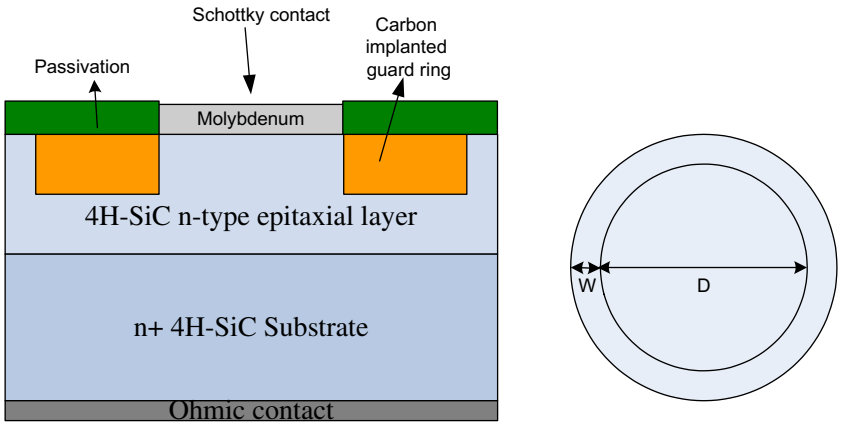

Fig. 1. The cross-sectional diagram of fabricated Mo/4H–SiC SBD.

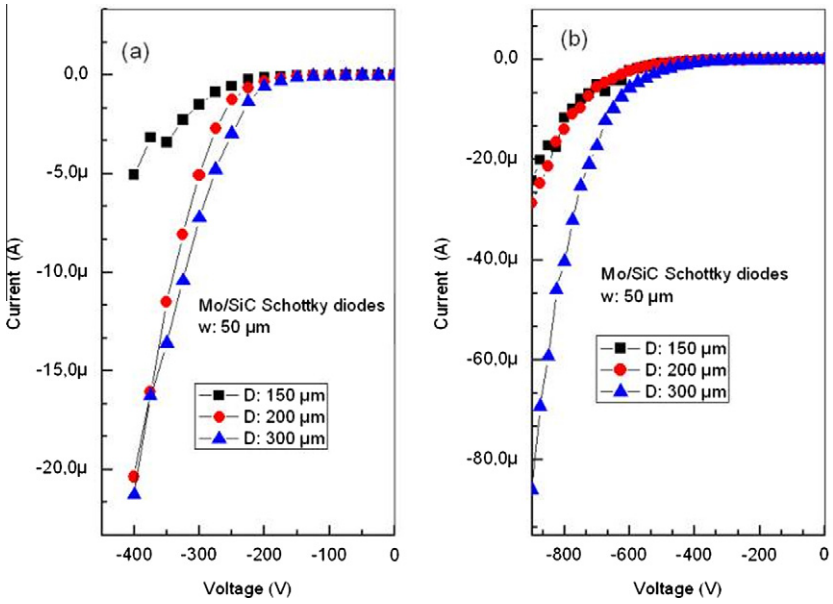

Fig. 2. Reverse *I–V* characteristics of Mo/4H–SiC SBD with different contact area at fixed widths of the guard ring at carbon dose of (a) $1.2 \times 10^{12}\,cm^{-2}$ and (b) $1.75 \times 10^{14}\,cm^{-2}$.

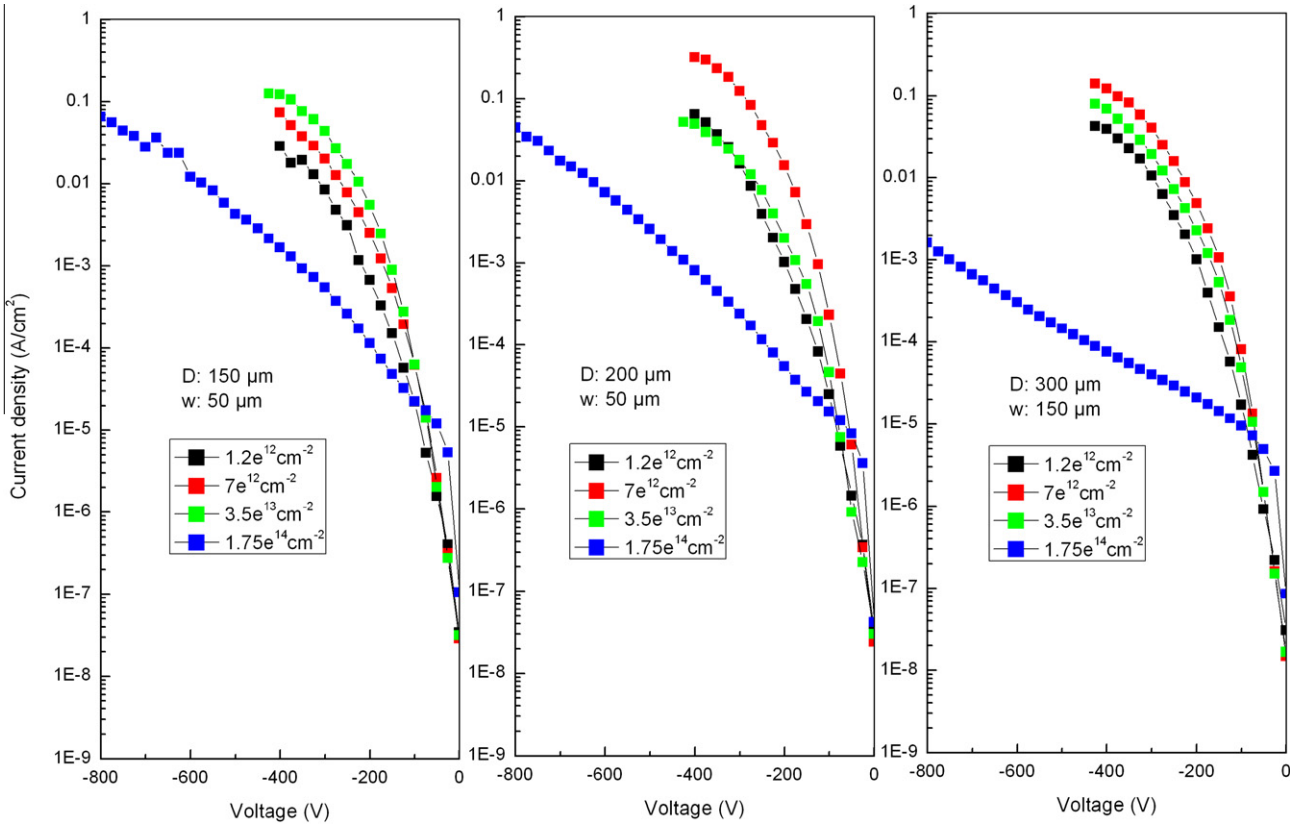

Fig. 3. Reverse current density–voltage curve of Mo-Schottky diodes with C-implanted guard ring for different ion implantation doses.

Note that, narrow guard-ring width is more favorable for switching characteristics [27].

In order to determine the relative importance of thermionic emission to field emission (tunneling) it is necessary to calculate the magnitude of the parameter E_{00} given by [28]

$$E_{00} = \frac{h}{4\pi}\left[\frac{N_d}{m^*\varepsilon_s}\right]^{1/2} = 1.86 \times 10^{-11}\left[\frac{N_d}{\varepsilon_r(m^*/m_0)}\right]^{1/2} eV \quad (1)$$

where h is the Planck constant, m_0 the free electron mass, m^* is the effective mass of electrons in the semiconductor, ε_r its permittivity and the donor concentration N_d is expressed in cm^{-3}.

In our case, (n-type 4H–SiC), and at our maximum doping level of $1.3 \times 10^{16}\,cm^{-3}$, $m^* = 0.2$, m_0 [9] and $\varepsilon_r = 9.7$, E_{00} was found to be about 1.52 meV.

The size of E_{00} with respect to kT gives an indication of the relative importance of thermionic-field emission to thermionic

emission. A comparison of E_{00} to the thermal energy kT shows thermionic emission to dominate ($E_{00}/kT = 0.058$).

However, under strong reverse bias which can cause the potential barrier to become thin, tunneling through the barrier may be significant on the reverse direction than in the forward direction [6,28].

The leakage current as a function of the implantation dose for different structures is shown in Fig. 3. For C-implantation doses of 1.75×10^{14} cm^{-2}, a significant reduction of the leakage current and an obvious improvement in the breakdown behavior is observed. The increase in the C-implantation doses results in a higher breakdown voltage of the diode due to a reduction of the electric field density within the SiC near the edge of the device. It seems that at lower implantation doses, field enhancement took place and affected the reverse current and breakdown behavior of the diodes [8].

These effects need further investigations to understand their physical mechanism.

3.2. Forward characteristics

3.2.1. Standard model

Typical forward I–V characteristics of a Mo/4H–SiC diodes measured at room temperature are shown in Fig. 4. All Schottky contacts exhibited a similar forward I–V characteristics behavior with a wide linearity region over several orders of magnitudes. However, for C-implantation doses of 1.75×10^{14} cm^{-2}, a significant reduction of the saturation current is observed. This suggests that there is a correlation between the carbon dose implantation and the Schottky barrier height.

From the forward I–V characteristics of the Mo/4H–SiC SBD measured at room temperature, Schottky diode parameters such as barrier height (Φ_{B0}), ideality factor (n), and series resistance (R_s) were determined.

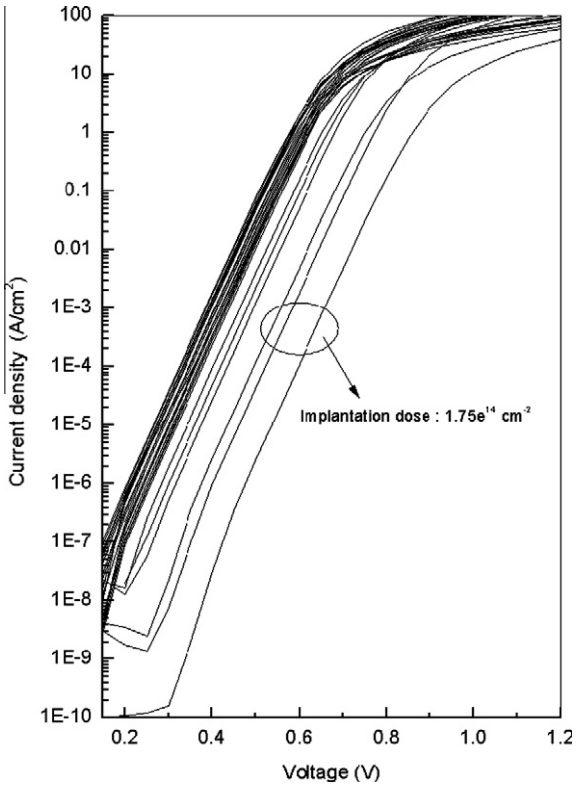

Fig. 4. Forward I–V curves of SBDS of various size measured at room temperature.

First, the electrical forward I–V measurements are analyzed using the standard thermionic emission–diffusion (TED) theory. The current through a homogeneous SBD at a forward bias V is described within the TED theory by [28]

$$I = I_s\left[\exp\left(\frac{\beta}{n}(V - R_s I)\right) - 1\right] \tag{2}$$

With the saturation current I_s defined by

$$I_s = AA^*T^2\exp(-\beta\Phi_{B0}) \tag{3}$$

Where A is the area of the diode, $\beta = q/kT$ with k the Boltzmann's constant, q the electron charge, T the absolute temperature and A^* the Richardson constant.

The ideality factor n, the saturation current I_s and the series resistance R_s were determined simultaneously by fitting the I–V curves using the so-called vertical optimization method [29] in which the theoretical value of A^* for 4H–SiC was taken 146 A/cm^{2}K^2 [3]. Review, tests, comments on the strengths and weaknesses of several methods for the determination of the diode parameters have been presented by Bashahu and Nkundabakura [30].

Both effective barrier heights and ideality factors vary from diode to diode. The SBH (Φ_{B0}) for Mo/4H–SiC has ranged from 0.97 to 1.17 eV and the ideality factor (n) from 1.02 to 1.11. The series resistance takes values between 7 and 23 Ω mainly due to slightly higher conductive substrate.

Therefore, in spite of the almost ideal behavior of the Mo/SiC contact observed at room temperature, idealities $n \approx 1$, in I–V curves and the non saturation of the reverse current can suggest that an inhomogeneous barrier is present in Mo/4H–SiC interface.

3.2.2. The barrier height inhomogeneity

The TED model treats the interface between the metal and the semiconductor as atomically flat and spatially homogeneous. However, it is now well established that Schottky potential barriers of a number of systems are generally not homogeneous. There are several physical reasons to include barrier fluctuation into the analysis of the transport measurement on Schottky diodes, like crystal defects, nonuniformity in the interfacial charges, and spatial distribution of the doping atoms [18,31,32].

Two approaches are generally used to describe inhomogeneous Schottky barriers [18,33]. In Werner's approach [33], the barrier height is supposed to be distributed according to a Gaussian type function which will usually lead to an apparent BH that is both temperature and bias dependent. However, Tung [18] considers in his model the presence of locally non uniform regions or patches with relatively lower or higher barriers with respect to an average barrier height. The interaction of the high barrier and low barrier is described with the help of the so called "saddle point".

In order to gain insight into the Schottky barrier and further justify the possibility of applying Tung's model [18] to our data, the temperature dependence of the Schottky barrier height and the ideality factor are examined.

Fig. 5 shows the forward I–V characteristics of the Mo/4H–SiC SBD measured at different temperatures ranging from 303 to 498 K. I–V curves represent the general electrical trend of the contact. These extracted parameters are both temperature dependent. The barrier height shows an increase with temperature and the ideality factor n follows a temperature behavior already observed and referred to as the "T_0 anomaly" [18,33,34].

We report the plot of nkT/q versus kT/q in Fig. 6 where the straight line describes the ideal behavior ($n = 1$). As can be seen from the figure, the experimental data could be fitted by a straight line parallel to that of the ideal case. According to Saxena [34], such

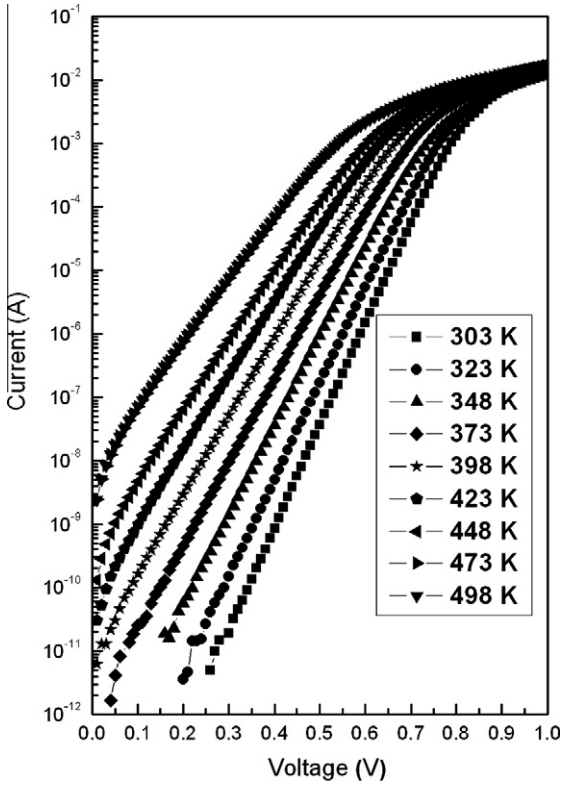

Fig. 5. Forward experimental *I–V* curves of Mo/4H–SiC diode at different temperatures.

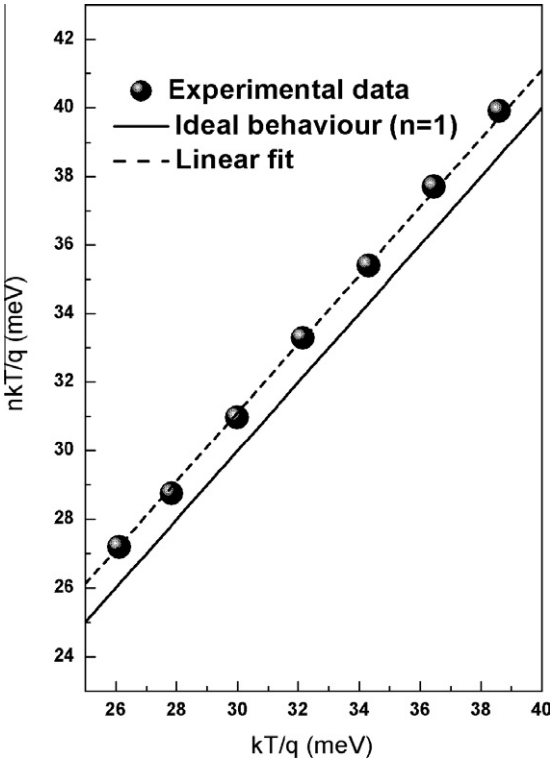

Fig. 6. Plot of *nkT* versus *kT* showing the T_0 effect.

behavior is typical to a SBD displaying the so called "T_0 *effect*" which means that the ideality factor can be expressed in the form

$$n(T) = 1 + \frac{T_0}{T} \tag{4}$$

Fig. 6 shows that the experimental results of $n(T)$ fit very well with the theoretical Eq. (4) with T_0 = 20.95 K. This value is in agreement with T_0 values obtained on SiC Schottky diodes [9]. Sullivan et al. [31] have shown that the "T_0 *effect*" is typical to SBD with a distribution of barrier inhomogeneities. So the possibility of applying Tung model to our data is justified. Indeed the presence of barrier inhomogeneities in 4H–SiC diodes [8,9,19,35] was already demonstrated by using the model of Tung.

High-temperature forward data can also used to obtain the Richardson constant and the average Schottky barrier height. Eq. (3) can be rewritten as

$$\ln(I_s/T^2) = \ln(AA^*) - (q/kT)\Phi_{B0} \tag{5}$$

Hence, the Richardson constant A^* can be determined from the intercept of $\ln(I_s/T^2)$ versus q/kT plot. The experimental data yield activation energy of 1.12 eV and a Richardson constant value 21.21 $Acm^{-2}K^{-2}$. The Richardson constant values are much lower than the known theoretically value of 146 $Acm^{-2}K^{-2}$. As will be discussed later, the deviation in the Richardson constant A^* was often identified in metal semiconductor interface inhomogeneity [36].

As mentioned above, Tung considered well-separated microdiodes or 'patches' characterized by low barriers embedded in a background of homogeneous higher uniform barrier height Φ_{bH}, which is independent of applied potential. The patches are taken to be small relative to the size of the depletion region such that the interaction of the patch with the surrounding depletion region causes a pinch-off or saddle point in the potential barrier away from the interface.

The patches and their distribution are obviously dependent on diode parameters and the contact fabrication process.

For an area density of patches with an assumed Gaussian distribution of γ (γ is a region parameter measuring the strength of the interface inhomogeneity), the total current is then given by [18]

$$I_T = AA^*T^2 \exp(-\beta\Phi_{BH})[\exp(\beta(V - R_sI_T)) - 1] \times \left[1 + \frac{8\pi\rho_p\eta^{1/3}\sigma^2}{9V_{bb}^{1/3}} \exp\left\{\frac{\beta^2\sigma^2V_{bb}^{2/3}}{2\eta^{2/3}}\right\}\right] \tag{6}$$

σ is the standard deviation of the distribution of γ given by a probability density function $N(\gamma)$

$$N(\gamma) = \frac{\rho_p}{\sqrt{2\pi\sigma}} \exp\left(-\frac{\gamma^2}{\sigma^2}\right) \tag{7}$$

Where ρ_p the density of patches ($\rho_p = N_p/A$, where N_p is the patch number), η, the doping parameter, $\eta = \varepsilon_s/qN_D$ (ε_s the permittivity and N_D the doping concentration), V_{bb} the band bending and V_n the bulk potential, $V_n = \beta ln(N_c/N_D)$, (N_c density of states in conduction band).

In order to get some more details about the inhomogeneity of these MS contacts, a fitting according to Eq. (6) can be applied to the *I–V* measurements, using Φ_{bH}, N_p, γ and R_s as adjustable parameters.

The obtained significant parameters Φ_{bH}, N_p, γ, R_s ruling the current transport are shown in Table 2.

A mean barrier height range from 1.2 to 1.39 *eV* has been obtained. This value is in overall agreement with the works presented previously [14–16], even if the Mo barrier heights reported by other groups are higher [13].

From this table, it can be seen that the homogeneous barrier is nearly the same for all diodes while the SBH determined from Eq. (2) are lower in agreement with the fact that according to thermionic theory the main part of the current will flow through patches with a low SBH [37].

Table 2
The fitting parameters Φ_{bH}, N_p, γ and R_S calculated from the room temperature *I–V* characteristics of all Mo/SiC diodes. The values obtained from the fit of Eq. (6) to the data are the range of the homogeneous BH, the standard deviation, the number of patches and the series resistance.

Carbon dose (cm^{-2})	Homgeneous barrier height Φ_{bH} (*eV*)	Number of patch N_p	Patch strength $\gamma(cm^{2/3}V^{1/3})$	Series resistance R_s (Ω)
1.2×10^{12}	1.22–1.33	3.4×10^{10}–6.5×10^{10}	5.4×10^{-5}–6.9×10^{-5}	7.86–22.79
7×10^{12}	1.21–1.34	2.2×10^{10}–6.7×10^{10}	4.5×10^{-5}–6.2×10^{-5}	7.97–17.44
35×10^{12}	1.22–1.28	4.5×10^{10}–6.6×10^{10}	4.27×10^{-5}–5.28×10^{-5}	8.24–11.79
175×10^{12}	1.2–1.39	3.27×10^{9}–9.5×10^{9}	5.21×10^{-5}–5.7×10^{-5}	8.33–17.85

The standard deviation parameter σ is determined to be $4.5 \times 10^{-5}\,cm^{2/3}V^{1/3}$ and $6.9 \times 10^{-5}\,cm^{2/3}V^{1/3}$ for the diodes and is almost constant. As the strength parameter σ of a given patch is related to its radius, this indicates that the carbon implantation dose does not strongly affect the patch radius. From Table 2 one can also see that the number of patches N_p decreases with increasing the Carbon implantation dose. In our results, the carbon implantation dose seems to reduce the number of patch and this presumably affects the SBH.

3.2.3. Discussion

The electronic transport in metal/SiC contacts is of great importance, and the exact description of the forward and the reverse characteristics is still in issue. Control of the Schottky-barrier height is of importance in minimizing the power loss.

A careful search in literature reveals that Mo/SiC has been investigated on both 4H and 6H polytypes. SBDs previously published data have been collected in Table 3.

From the listed values, the Schottky barrier heights obtained for the same metal under different experimental conditions are significantly different. This difference can be attributed to the different conditions of preparation of the devices i.e. the quality of the semiconductor, surface preparation, the morphology of the surface, the edge of termination used and also the temperature of annealing. In fact, it has been reported that in the case of molybdenum the Schottky barrier height increase with increasing temperature annealing [14].

However, the homogeneous SBH (using Tung's model) value obtained is this work, is very close to the theoretical SBH $\Phi_B = \Phi_m - \chi$ of about 1.23 *eV* expected for the Mo/4H–SiC SBH obtained by considering the Molybdenum work function, $\Phi_m = 4.53$ *eV* [38], and the usually used value of the electron affinity of 4H–SiC, $\chi = 3.3$ *eV*. Note that the work function of the metal can be anisotropic.

Table 3
Schottky barrier heights for different Mo/SiC diodes. Data are collected from different groups.

	$\Phi_B/_{CV}$	$\Phi_B/_{IPE}$	$\Phi_B/_{IV}$	Obs.	Refs.
6H	1.3			Si face	[44]
6H	<1.2			Si face	[45]
6H	1.14			Si face	[46]
4H	1.03-	1.36		3.5° off-axis substrate, Si face	[4]
4H			1.05	Guard ring, 500 °C anneal	[8]
4H	1.66	1.27	1.3	Si face	[13]
4H	2.25	1.64	1.6	C face	[13]
4H			1.2–1.3	Three zone JTE, 600 °C anneal	[14]
4H			1.21–1.3	B implanted JTE, 400 °C anneal	[15–16]
4H	1.08		1.04	JTE, No annealing	[17]

As indicated earlier, it is important to note that the extracted value of the effective Richardson constant has been found to be several orders of magnitude lower than the theoretically predicted value ($146\,Acm^{-2}K^{-2}$). The discrepancy between the theoretical and experimental value of A^* has already often reported in literature and observed when analyzing SiC Schottky diodes and many efforts have been done in the last years to explain and model the Schottky contacts on SiC, trying to accord experimental data to the theoretical value [6,9,10,36]. The exact value of Richardson's constant for SiC SBDs has been debated by many authors [6,9,12,36]. The underestimation of the Richardson's contact in SiC, can then be attributed to an effective area involved in the current transport which may be significantly lower than the geometric area of the contact, thus finding its ultimate physical reason in the quality of the metal semiconductor/interface [9]. The more plausible causes may be indicated in the presence of surface defects in the material, interface roughness and processing-induced contaminations of the surface [6,9,36].

The lower value of experimentally determined Richardson constant indicates that the effective active area is in fact much smaller than the device area, which must be included in the calculation for the Richardson constant [9]. To explain these discrepancies, according to Eq. (6), and following the procedure developed by Roccaforte et al. [9] for the determination of the modified Richardson constant we get

$$I_T \approx AA^*T^2\left[\frac{8\pi\rho_p\eta^{1/3}\sigma^2}{9V_{bb}^{1/3}}\exp\left\{\frac{\beta^2\sigma^2V_{bb}^{2/3}}{2\eta^{2/3}}\right\}\right] \times \exp(-\beta\Phi_{BH})[\exp(\beta(V-R_sI_T))-1] = I_{sm}[\exp(\beta(V-R_sI_T))-1] \quad (8)$$

The intercept at the ordinate of the modified $\ln(I_{sm}/T^2)$ vs $1/kT$ plot shown in Fig. 7 gives the Richardson constant A^* as 96.03 A/cm^2 K^2. The obtained Richardson constant value is relatively in close agreement with the value of 146 A/cm^2 K^2 known for *n*-type 4H–SiC.

Although the analysis of the *I–V* analysis data provides an indirect evidence of barrier inhomogeneities at the Mo/SiC interface, the method does not directly give information on the quality of the surface/interface. In 4H–SiC, it has been shown that defects exist both in the substrates and overgrown epilayers [39]. Identification of defects in SiC, their densities, their correlations with electrical properties, and ways to reduce them is a very active area of research at present [11,22,32,40–42]. Recently, it has been shown that micropipes can affect seriously the barrier height and the breakdown voltage of the device [42]. Lee and Capano [41] have shown the existence of correlation between the reverse breakdown and the surface defects of Ni/4H–SiC Schottky barrier diodes. Also, growth pits were proposed as source defects to understand the Schottky barrier inhomogeneities [11].

The presented results support the conclusion that the SBH inhomogeneities and excess leakage current may be caused by the defects located in substrate or at the interface.

Moreover, it is known that molybdenum can readily react with the SiC to form a silicide, when reacted with elemental Si and form carbide when reacted with elemental C, and show little added reaction when performing an annealing up to 800 °C [43]. The evidence thus indicates that reactions and the creation of new phases (Mo_2C, $MoSi_2$, Mo_3Si), can increase the barrier height and lead to significant inhomogeneity due to a mixture of different phases at the M–S interface.

To sum up, excess leakage current and SBH inhomogeneites are influenced by the presence of surface defects in the material and the interface roughness due to the existence of a mixture of different phases [31,32]. It would also be of interest to further investigate how the defects affect the Schottky diode parameters.

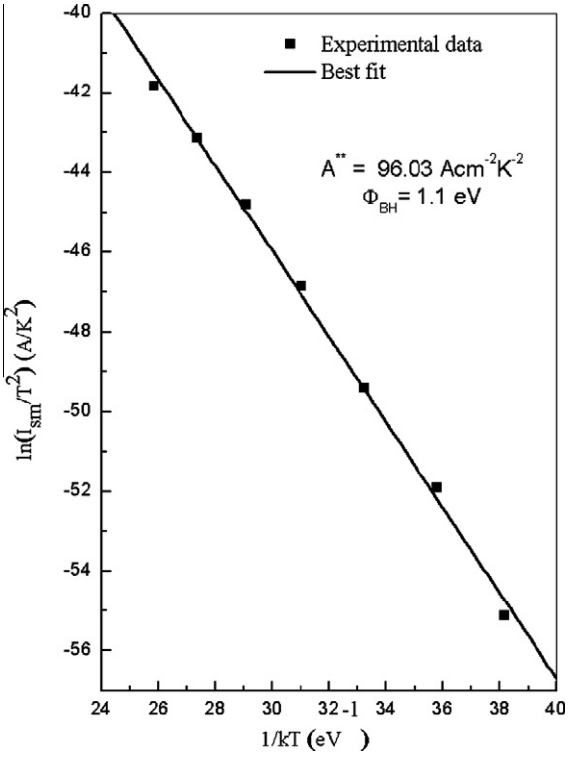

Fig. 7. "Modified" Richardson plot $\ln(I_{sm}/T^2)$ vs $1/kT$. A value of 96.03 A/cm^2 K^2 for the Richardson's constant could be determined by the intercept of the linear fit of the data.

4. Conclusion

Molybdenum SBDs fabricated on *n*-type 4H–SiC with different areas and with different edge termination have been investigated by current–voltage measurements at different temperatures. Both effective barrier heights and ideality factors vary from diode to diode. The results reported in the present paper substantiate published results in literature and support the conclusion that defects determine the leakage current and breakdown voltage.

The barrier inhomogeneity has been taken into account by assuming the pinch off model of the barrier height and consequently much more consistent values of the SBHs are obtained compared to those previously published data on Mo/4H–SiC diodes. Also, a correlation between the number of patches N_p (defects) and the Carbon implantation dose has been obtained. The Carbon implantation dose seems to reduce the density of patches and this presumably increases the SBH.

Although, the experimental results reported in the present work shed some light on some properties of the Mo/4H–SiC Schottky diodes, it also suggests that further microstructural analysis of the Mo-SiC interface as well as rigorous modeling are needed to elucidate the reverse leakage behavior [44–46].

Acknowledgments

The authors would like to thank Dr. V. Haublein and C. Ellig from Franhaufer Institute, Erlangen for their support during device characterization.

References

[1] J. Baliga, Silicon Carbide Power Devices, World Scientific, 2005.
[2] M. Shur, S. Rumyantsev, M. Levinshtein, SiC Materials and Devices, World Scientific, 2006.
[3] A. Itoh, H. Matsunami, Phys. Stat. Sol. (a) 162 (1997) 389.
[4] R. Yakimova, C. Hemmingsson, M.F. Macmillan, T. Yakimov, E. Janzén, J. Electron. Mat. 27 (1998) 871.
[5] V. Saxena, J.N. Su, J. Andrew, A.J. Steckl, IEEE Trans. Electron. Dev. 46 (1999) 456.
[6] B.J. Skromme, E. Luckowski, K. Moore, M. Bhatnagar, C.E. Weitzel, T. Gehoski, D. Ganser, J. Electron. Mat. 29 (2000) 376.
[7] M. Treu, R. Rupp, H. Kapels, W. Bartsch, Mater. Sci. Forum 353–356 (2001) 679.
[8] R. Weiss, L. Frey, H. Ryssel, Appl. Surf. Sci. 184 (2001) 413.
[9] F. Roccaforte, F. La Via, V. Raineri, R. Pierobon, E. Zanoni, J. Appl. Phys. 93 (2003) 9137.
[10] J.M. Bluet, D. Ziane, G. Guillot, D. Tournier, P. Brosselard, J. Montserrat, P. Godignon, Superlattices Microstruct. 40 (2006) 399.
[11] X. Ma, P. Sadagopan, T.S. Sudarshan, Phys. stat. sol. (a) 203 (2006) 643.
[12] M.E. Aydın, N. Yıldırım, A. Türüt, J. Appl. Phys. 102 (2007) 043701.
[13] O. Shigiltchoff, S. Bai, R.P. Devaty, W.J. Choyke, T. Kimoto, D. Hobgood, P.G. Neudeck, L.M. Porter, Mater. Sci. Forum 433–436 (2003) 705.
[14] T. Nakamura, T. Miyanagi, I. Kamata, T. Jikimoto, H. Tsuchida, IEEE Electron. Dev. Lett. 26 (2005) 99.
[15] K. Vassilevski, I. Nikitina, P. Bhatnagar, A. Horsfall, N. Wright, A.G. O'Neill, M. Uren, K. Hilton, A. Munday, A. Hydes, C.M. Johnson, Mater. Sci. Forum 527–529 (2006) 931.
[16] A. Vassilevski, I. Nikitina, A. Horsfall, N.G. Wright, A.G. O'Neill, K.P. Hilton, A.G. Munday, A.J. Hydes, M.J. Uren, C.M. Johnson, Mater. Sci. Forum 556–557 (2007) 873.
[17] D. Perrone, M. Naretto, S. Ferrero, L. Scaltrito, C.F. Pirri, Mater. Sci. Forum 615–617 (2009) 647.
[18] R.T. Tung, Phys. Rev. B 45 (1992) 13509.
[19] S. Nigam, J. Kim, B. Luo, F. Ren, G.Y. Chung, S.J. Pearton, J.R. Williams, K. Shenai, P.G. Neudeck, Solid State Electron 47 (2003) 57.
[20] S. Maximenko, S. Soloviev, D. Cherednichenko, T. Sudarshan, J. Appl. Phys. 97 (2005) 013533.
[21] P.G. Neudeck, J.A. Powell, IEEE Electron. Dev. Lett. 15 (1994) 63.
[22] P.G. Muzykov, A.V. Bolotnikov, T.S. Sudarshan, Solid State Electron 53 (2009) 14.
[23] K.J. Schoen, J.M. Woodall, J.A. Cooper Jr., M.R. Melloch, IEEE Trans. Electron. Dev. 45 (1998) 1595.
[24] C. Blasciuc-Dimitriu, A.B. Horsfall, N.G. Wright, C.M. Johnson, K.V. Vassilevski, A.G. O'Neill, Semicond. Sci. Technol. 20 (2005) 10.
[25] P. Brosselard, N. Camara, V. Banu, X. Jorda, M. Vellvehi, P. Godignon, J. Millan, IEEE Trans. Electron. Dev. 55 (2008) 1847.
[26] H. Saitoh, T. Kimoto, H. Matsunami, Mater. Sci. Forum 457-460 (2004) 997.
[27] K. Ueno, T. Urushidani, K. Hashimoto, Y. Seki, IEEE Electron. Dev. Lett. 16 (1995) 331.
[28] E.H. Rhoderick, R.H. Williams, Metal-Semiconductor Contacts, 2nd ed., Clarendon, Oxford, 1988.
[29] A. Ferhat Hamida, Z. Ouennoughi, A. Hoffmann, R. Weiss, Solid State Electron 46 (2002) 615.
[30] M. Bashahu, P. Nkundabakura, Solar Energy 81 (2007) 865.
[31] J.P. Sullivan, R.T. Tung, M.R. Pinto, W.R. Graham, J. Appl. Phys. 70 (1991) 7403.
[32] D.J. Ewing, Q. Wahab, R.R. Ciechonski, M. Syvajarvi, R. Yakimova, L.M. Porter, Semicond. Sci. Technol. 22 (2007) 1287.
[33] J.H. Werner, H.H. Güttler, J. Appl. Phys. 69 (1991) 1522.
[34] A.N. Saxena, Surf. Sci. 13 (1969) 151.
[35] H.-J. Im, Y. Ding, J.P. Pelz, W.J. Choyke, Phys. Rev. B 64 (2001) 075310.
[36] C.F. Pirri, S. Ferrero, L. Scaltrito, D. Perrone, S. Guastella, M. Furno, G. Richieri, L. Merlin, Microelectron. Eng. 83 (2006) 86.
[37] S. Forment, M. Biber, R.L. Van Meirhaeghe, W.P. Leroy, A. Turut, Semicond. Sci. Technol. 19 (2004) 1391.
[38] D.R. Lide, CRC Press, Boca Raton, FL, 2005.
[39] W. Chen, K.Y. Lee, M.A. Capano, J. Crystal Growth 297 (2006) 265.
[40] Y. Wang, G.N. Ali, M.K. Mikhov, V. Vaidyanathan, B.J. Skromme, B. Raghothamachar, M. Dudley, J. Appl. Phys. 97 (2005) 013540.
[41] K.-Y. Lee, M.A. Capano, J. Electron. Mat. 36 (2007) 272.
[42] M.L. Bolen, J. Capano, J. Electron. Mat. 38 (2009) 574.
[43] K.M. Geib, C. Wilson, R.G. Long, C.W. Wilmsen, J. Appl. Phys. 68 (1990) 2796.
[44] A.L. Syrkin, A.N. Andreev, A.A. Lebedev, M.G. Rastegaeva, V.E. Chelnokov, J. Appl. Phys. 78 (1995) 5511.
[45] A.L. Syrkin, A.N. Andreev, A.A. Lebedev, M.G. Rastegaeva, V.E. Chelnokov, Mater. Sci. Eng. B 29 (1995) 198.
[46] A.L. Syrkin, J.M. Bluet, G. Bastide, T. Bretagnon, A.A. Lebedev, M.G. Rastegaeva, N.S. Savkina, V.E. Chelnokov, Mater. Sci. Eng. B 46 (1997) 236.